https://doi.org/10.48048/tis.2024.7262

Adsorption of Congo Red from Aqueous Solutions by Alginate-Nanocellulose-Polyethyleneimine Hydrogel Beads

Putri Amanda[1,*], Yudhi Dwi Kurniawan[2], Kurnia Wiji Prasetiyo[1], Fahmi Hasan[1] and Anita Amelia[3]

[1]Research Center for Biomass and Bioproduct, National Research and Innovation Agency, Central Jakarta, Indonesia
[2]Research Center for Pharmaceutical Ingredient and Traditional Medicine, National Research and Innovation Agency, Central Jakarta, Indonesia
[3]Environmental and Industrial Hygiene Division, Petrolab Services, Daerah Khusus Ibukota Jakarta, Indonesia

([*]Corresponding author's e-mail: putri.amanda@brin.go.id)

Received: 1 July 2023, Revised: 9 August 2023, Accepted: 17 August 2023, Published: 1 October 2023

Abstract

Biobased adsorbents have been developed for the removal of dye contaminants in aqueous solution. Hydrogel beads from alginate containing TEMPO-oxidized cellulose nanofibers (TOCNF) grafted with polyethyleneimine (PEI), namely Al/TOCNF-PEI, were prepared and evaluated as a new adsorbent for Congo Red (CR). The Al/TOCNF-PEI hydrogel beads were made with various concentrations of TOCNF/PEI, the optimum concentration is 45 wt% or Al/TOCNF-PEI45. The hydrogel was characterized by using Fourier-Transform Infrared spectroscopy and Scanning Electron Microscopy. The adsorption performance of the Al/TOCNF-PEI hydrogel beads towards CR was investigated in terms of changing of TOCNF-PEI content, initial concentration, pH, contact time, and adsorbent dosage. The maximum capacity of the adsorbent for CR was found to be 9.437 mg/g at the optimal conditions (pH = 3; T = RT) with the removal efficiency reaching 95 %. This result was ascribed to occur due to the electrostatic attraction between the protonated hydroxyl group and ammonium moiety of the hydrogel beads and the anionic sulfonate group of the CR. Upon fitting the adsorption data, the adsorption mechanism was consistent with the Freundlich isotherm and pseudo-second-order kinetic models. Based on this finding, the low-cost Al/TOCNF-PEI45 hydrogel beads demonstrated a great potential for the removal of hazardous dyes in wastewater.

Keywords: Dyes, Composite beads, Alginate, Adsorption, Congo Red, Wastewater

List of abbreviations

CR : Congo Red
MB : Methylene Blue
TOCNF : TEMPO-oxidized cellulose nano fibers (TOCNF)
PEI : Polyethylenimine
Al/TOCNF-PEI : Alginate- TEMPO-oxidized cellulose nanofibers (TOCNF) Polyethyleneimine
Al/TOCNF-PEI45 : Alginate with 45 wt% of TEMPO-oxidized cellulose nanofibers (TOCNF) Polyethyleneimine

Introduction

Organic dye is one of the many hazardous materials that is discharged into the environment because of rapid industrialization and enormous population growth occurring simultaneously [1]. Synthetic chemicals known as organic colorants or dyes have widespread application in the textile and cosmetics industries, as well as in the manufacture of paper and plastics manufacture. Textile dyes as one of the largest environmental pollutants severely diminish the aesthetic appeal of water bodies, raise BOD and COD levels, inhibit photosynthesis, stunt the plant growth, infiltrate the food chain, and may even be poisonous, mutagenic, or carcinogenic. The presence of dyes in the environment is not only detrimental to human health but also to the health of ecosystems [1-3].

Azo dyes compose more than 90 % of organic colorants, and they are now a commonly used synthetic color. One of the most notable examples of azo dyes is the sodium salt of 3,3′-([1,1′-biphenyl]-4,4′-diyl) bis (4-aminonaphthalene-1-sulfonic acid), which is also known as Congo Red (CR) in industry. CR has broad application in various sectors such as timber, coloring agents, fabrics, dyestuffs, plastic, printing, and many more. The CR dye is carried into the water supply by a number of different industrial effluents. CR is naturally poisonous and poses a risk to the health of both human beings and animals [4,5]. Because of the associated great structural stability, CR exhibits a high level of resistance. In humans, CR is responsible for a variety of health problems, including anorexia, weakness, and irritation of the gastrointestinal tract. Because CR is a benzidine-based dye, there is a possibility that it might cause cancer as well as genetic mutations [5,6]. Hence, there have been great efforts to remove this pollutant from water bodies.

Extensive research has been conducted to develop the technique of removing ago dyes from aqueous solutions, and several physical and chemical procedures for cleaning water from these chemicals have been developed. These procedures include photocatalysis [7], filtration [8], ozonation [9], and adsorption [10,12]. The latter is regarded as one of the most advantageous methods for the removal of dyes among others due to the fact that its operation is straightforward and effective, and the adsorbent may be recycled and reused.

The most well-known approach for eliminating pollutants from surface water or sewage is adsorption. The low cost and adaptability of adsorption strategy make this approach superior for color removal. In addition, this technique does not generate any hazardous by-products following the removal of the target component [11,13,14].

The removal of CR from wastewater has been accomplished using a wide range of adsorbents such as immobilized *Aspergillus niger* on alginate [15], membrane of polyvinyl alcohol/sodium alginate/ZSM-5 zeolite [5], Mg/Al layered [16] and dialdehyde cellulose beads crosslinked with chitosan [6]. Adsorbents that are inexpensive, abundant, non-toxic, biodegradable, and beneficial to the environment are highly desirable, but their development remains a big challenge. In this regard, biopolymer adsorbent has emerged as a novel type of adsorbent to be applied in the treatment of wastewater [17].

Alginate is a biopolymer containing linear, unbranched, and naturally occurring polysaccharide co-polymer. It comprises 1,4-linked β-D-mannuronic acid (M-block) and α-L-glucuronic acid (G-block), both of which may be found in a variety of different compositions and sequences [5,17]. Alginate is a seaweed-derived linear carboxylate polymer and has both carboxylic and hydroxyl groups, making this material highly water friendly. Alginate may bind to divalent ions to produce hydrogel beads. Hydrogels are 3-dimensional networks of polymers and made from natural or man-made materials that can hold or absorb a lot of water or biological fluids. Hydrogels made of calcium alginate could be used as adsorbents because of its low price, nontoxicity, strong water affinity, and biocompatibility to living things [17,19]. Asadi *et al.* 2018 reported alginate-based hydrogel beads efficiently adsorbed Methyl Violet (MV) from aqueous solution [17]. Abou-Zeid *et al.* 2021 using bio composite of alginate to remove heavy metal in aquous solution and the biocomposite beads exhibited high efficiency towards removing of heavy metal ions; Cu^{2+}, Pb^{2+}, Mg^{2+}, and Fe^{2+}. These material consists of the biocomposite of alginate and nanocellulose (Alg-CNF, Alg-CNC, and Alg-TPC-CNF) [19].

Nanocellulose is a lightweight, solid material consisting of nano-sized fibrils. This material has been used in a variety of applications ranging from catalysis to water purification [20-22]. However, without structural modification, the adsorption capacity of unmodified nanocellulose is poor due to lack of strong binding sites for attracting contaminants such as heavy metals or dyes. Therefore, pure nanocellulose is not an ideal material to adsorb these species in a desirable level [23-25]. Nevertheless, many reported works demonstrated that grafting nanocellulose with branching polyethyleneimine (PEI) was a straightforward and inexpensive approach for adding amino functionality, which could improve the adsorption capacity of the resulting material. Zhang *et al.* in 2016 reported that TOCNF-PEI showed good heavy metal removal ability [26]. In addition, Guo *et al.* in 2017 also prepared PEI-functionalized cellulose aerogel beads which were highly effective for the removal of hexavalent chromium from aqueous solution [27].

In this work, we disclose our efforts to construct a biocomposite of alginate/TOCNF-polyethylenimine hydrogel beads through ionic-crosslinking of sodium alginate with calcium ions. To the best of our knowledge, utilization of alginate supported TOCNF-PEI for removal dyestuff has not been reported in the literature. These beads were then used as adsorbents for CR in aqueous media. Attenuated total reflectance (ATR) FTIR and SEM were applied to analyse the chemical structures and the surface morphologies of the sample, respectively. Evaluation of the adsorption characteristic of this adsorbent over CR was carried out in a variety of variables, including starting concentration of the CR dye, contact duration, pH, and adsorbent dose. For determining the capacity and adsorption mechanism of the adsorbent, isotherm and kinetic models were carried out.

Materials and methods

Material

All chemicals were used without prior purification. Sodium alginate, $CaCl_2$, polyethyleneimine (PEI) with an average MW of ~270.000 and Congo Red were purchased from Sigma Aldrich. The TEMPO-oxidized cellulose nanofibrils were prepared according to our previous work [28,29].

Preparation of TOCNF-PEI

The TOCNF-PEI was prepared following the step by (Zhang *et al.*, 2016) with little modification. In general, a TOCNF with 100 mL of methyl alcohol [26]. 10 g of PEI was added to the TOCNF suspension, which was stirred for 24 h to mix it well. After that, the mixture was spun at 8,000 rpm to get rid of any PEI left over. The precipitate was mixed right away into 100 mL of deionized water. Then, dropwise 4 mL of a 25 % glutaraldehyde solution was added, and the pH of the solution was changed to 8 with 0.4 M NaOH. The system was then stirred for 1 h so that TOCNF and PEI could crosslink. The product was eventually separated, carefully cleaned with deionized water, freeze-dried, and powdered to provide TOCNF-PEI.

Preparation of Al/TOCNF-PEI biocomposite beads

The alginate/TOCNF-PEI biocomposite beads were prepared by the following step: 2 g of alginate, TOCNF-PEI with various concentration (0, 5, 10, 15, 30, 45, 60 wt%) and distilled water were added to a beaker glass to make the total weight of 100 g. The mixture was stirred at 600 rpm and heated at 80 °C for 60 min until a transparent and homogeneous solution was formed. Adopting the ionotropic gelation technique reported in the literature [30], the hydrogel solution was loaded into a 10 mL syringe, dropped into a 5 % $CaCl_2$ aqueous solution with 10 cm from the solution surface. The mixture was stirred at 200 rpm. Hydrogel beads formed were left in $CaCl_2$ solution for 1 h to form a perfect gelation process. As a control, alginate beads without TOCNF-PEI were prepared by mixing 2 g of alginate and 98 g of distilled water.

Characterization of biocomposite beads

Physical characterization of biocomposite beads was evaluated in terms of diameter, moisture content, and syneresis. The diameter of the biocomposite beads was estimated using Mitutoyo digital caliper, while their moisture content was measured using Moisture Analyzer MOC63u. The syneresis of the biocomposite beads was determined by weighing the final gel after draining in room temperature for 24 h and gently wiping off excess water from the surface and comparing this value to the initial weight of biocomposite beads. The syneresis value was calculated by Eq. (1).

$$Syneresis\ (\%) = \frac{Wo - W}{Wo} x\ 100\% \quad (1)$$

W_o dan W were weights of beads before and after draining in room temperature for 24 h, respectively. For each data point, the measurement was replicated thrice.

The structure and chemical composition of the samples were characterized using FT-IR (Spectrum Two, Perkin Elmer, USA). The microscopic appearance of the samples was observed using FESEM (FE-SEM Thermo Scientific Quattro S) at an accelerating voltage of 1 kV. The concentration of adsorbate before and after adsorption was measured using UV-Vis Spectrophotometer (UV-Vis 800 Shimadzu, Japan) at λ_{max} = 497 nm.

Preliminary adsorption test

Two types of dyes, congo red and methylene blue, which represent anionic and cationic dyes were used to test the ability of biocomposite beads to remove the dyes in aqueous solution.

The adsorption experiments were carried out using 250 mL Erlenmeyer flask by inserting the adsorbent (10 g/L) into 100 mL of CR and MB dyes solution with concentration 100 mg/L. The mixture was stirred with an orbital shaker at 200 rpm in room temperature (RT) for 240 min.

Congo Red adsorption test

The adsorption of CR from aqueous solution onto Al/TOCNF-PEI beads biocomposite was evaluated through batch adsorption experiments. Before adsorption experiments were performed, a series of CR solutions with different concentrations were prepared using Ultrapure Water and then analyzed using a UV spectrophotometer, which recorded a characteristic absorption peak of CR at 497 nm.

Stock solution of CR (1,000 mg/L) was prepared by dissolving 1 g of CR dye in 1,000 mL of deionized water. The solution stock was then diluted to get the CR dye with various concentrations of 10, 20, 50, 100, 150 and 200 mg/L. To obtain the best adsorption capacity of Al/TOCNF-PEI adsorbents, TOCNF-PEI content in alginate was varied (0 - 60 % wt).

The adsorption experiments were carried out using 250 mL Erlenmeyer flask by inserting the adsorbent (10 g/L) into 100 mL of CR dye solution with variation in initial dye concentration (10 - 200 mg/L). The mixture was stirred with an orbital shaker at 200 rpm in room temperature (RT). The supernatant of the CR dye solution was sampled at different time intervals (0 - 240 min). The absorbance of CR was measured using a UV-Vis spectrophotometer. The concentration of CR was then calculated using a standard CR dye calibration curve. Then, the adsorption capacity of CR (qe = mg/g) was calculated using Eq. (2).

$$qe = \frac{(Co - Ce)}{m} x\ V \tag{2}$$

where, C_0 and C_e (mg/L) are the initial concentration and the remaining concentration after equilibrium, respectively. V (mL) is the volume of CR solution and m (mg) is the weight of Al/TOCNF-PEI beads. The percentage of dye removal was determined by Eq. (3).

$$Dye\ Removal\ (\%) = \frac{(Co - Ce)}{Co} x\ 100\% \tag{3}$$

The effect of pH was carried out using the initial dye concentration of 100 mg/L at RT. The effect of the adsorbent dosage (5, 10, 15 g/L) was carried out with the initial dye concentration of 100 mg/L, pH 6.0, and at RT. Other conditions were similar with the adsorption conditions set on the effect of the initial dye concentration.

Kinetic and isotherms study

To explain adsorption isotherms, 2 types of models are often used: The Langmuir and Freundlich models. Furthermore, 2 types of kinetic models were utilized in this work to explain the mechanism of the adsorption process: Pseudo-first order (PFO) and pseudo-second order (PSO). The Kinetic and Isotherm research was calculated at room temperature using adsorbent 10 g/L in 100 mL of CR solution with a concentration of 100 mg/. Spectrophotometry UV-Vis was used to determine the concentration of CR before and after adsorption.

Results and discussion

Preparation of hydrogel beads

The mechanism of our Al/TOCNF-PEI hydrogel beads is illustrated in **Figure 1**.

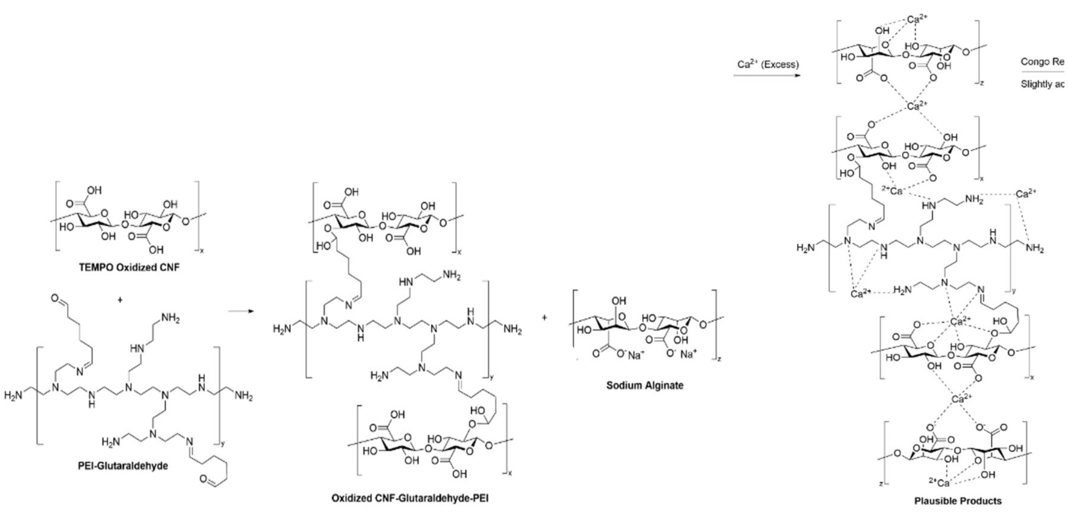

Figure 1 Reaction mechanism of Alginate/TOCNF-PEI hydrogel beads synthesis.

Initially, we prepared TOCNF-PEI using glutaraldehyde as a crosslinker. At first, the reactive aldehyde groups were formed through a reaction in alkaline condition. The carboxylate groups on the Tempo CNF surface react with the activated glutaraldehyde, creating covalent connections between the aldehyde groups of glutaraldehyde and the carboxylate groups of TOCNF. Simultaneously, the amino groups of PEI react with the remaining aldehyde groups of glutaraldehyde, forming imine or Schiff base linkages, producing TOCNF-PEI.

The FTIR spectrum of TOCNF, PEI, and TOCNF-PEI are displayed in **Figure 2**. The carbonyl stretching vibration of TOCNF was displayed by a peak centered at 1,606 cm^{-1} [29]. The shouldered peak located between 1,600 and 1,800 cm^{-1} in TOCNF-PEI spectrum seemed to be an overlap of 3 separated peaks, representing N-H bending at 1,615 cm^{-1}, C=O stretching of $-COO^-$ and -COOH at 1,660 and 1,710 cm^{-1}, respectively [26]. The effective incorporation of PEI into TOCNF in TOCNF-PEI was evidenced by the significant increase of C-C skeleton vibration at 1170 cm^{-1} as well as the emergence of $-CH_2$ stretching vibration at 2,903 and 2,829 cm^{-1} [26,28].

Further upon to produce alginate-TOCNF.PEI beads, the droplets of sodium alginate and oxidized CNF-glutaraldehyde-PEI mixture was immersed into 5 % of aqueous $CaCl_2$, solidification occurred forming round-shaped beads.

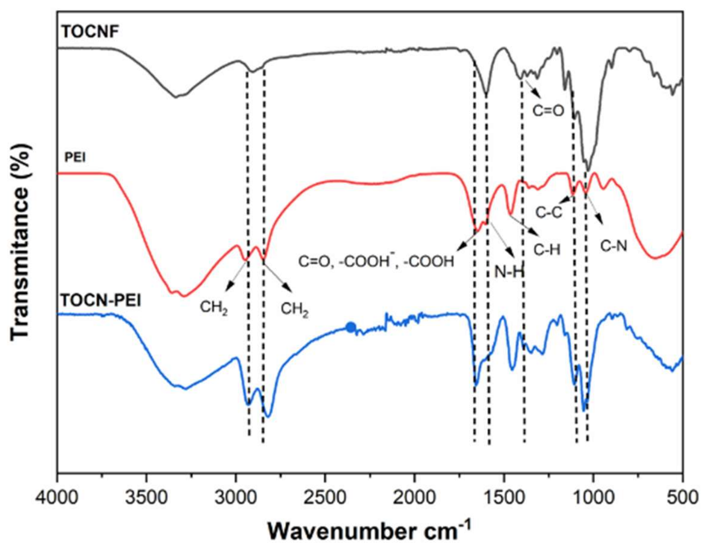

Figure 2 FTIR spectra of TOCNF, PEI and TOCNF-PEI.

Characterization of Al-TOCN/PEI hydrogel beads

The physical characteristics of the prepared biocomposite beads Al/TOCNF-PEI.

Table 1 Physical characteristic of beads.

Characteristic	Alginate	Al/TOCNF-PEI5	Al/TOCNF-PEI15	Al/TOCNF-PEI30	Al/TOCNF-PEI45	Al/TOCNF-PEI60
Diameter (mm)	3 - 3.2	2.9 - 3.1	3.1 - 3.2	2.8 - 3.2	2.9 - 3.2	3 - 3.2
Moisture content (%)	± 97	± 97	± 96	± 97	± 96	± 96
Syneresis (%)	29 ± 1.1	31 ± 1.5	33 ± 1.4	34 ± 1.3	34 ± 1.2	31 ± 1.3

Table 1 demonstrates that the diameter and moisture content of hydrogel beads are unaffected by the various TOCNF-PEI di concentrations. Moreover, in addition, both of hydrogel beads: Alginate and the biocomposite Alginate/TOCNF-PEI with various concentration of TOCNF PEI show low syneresis which refers to a condition where a hydrogel experiences minimal or insignificant shrinkage, resulting in minimal expulsion of water or solvent from its structure. In other words, in a variety of circumstances, such as changes in temperature, pH, or solvent concentration, a hydrogel with low syneresis maintains its volume and water content well.

Optimization of TOCNF/PEI concentration in bio composite beads for removing dyes

Before optimizing the concentration of TOCNF/PEI in alginate beads was carried out. The ability of bio composites beads to remove dyes in aqueous solution was evaluated using MB and CR. **Figures 3(a) - 3(b)** showed that the photograph of solution dyes after adsorption test after 240 min. the adsorbent did not affectively adsorb MB dyes in contrast with CR. Moreover, further adsorption studies were conducted using the anionic dye, Congo red.

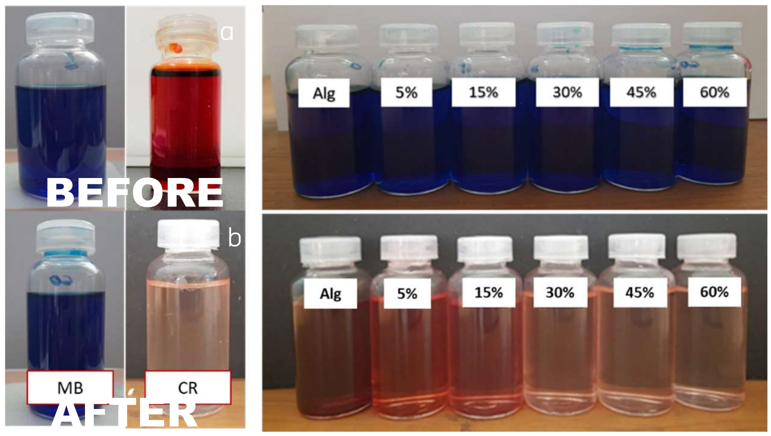

Figure 3 a. Photographs of MB and CR dye solutions before and after 240 min adsorption test using Al/TOCNF-PEI beads; b. the color change of MB and CR solutions after adsorption test prepared in various concentrations of TOCNF-PEI.

The concentration of TOCNF-PEI used to prepare Al/TOCNF-PEI adsorbent for CR was varied to obtain the best performance, which was evaluated by measuring the adsorption capacity (qe) and dye removal (%). The adsorption test was carried out using 10 g/L of adsorbent and 100 mg/L of CR at room temperature (RT) for 240 min pH 6. The beads made of alginate hydrogel were utilized as a control. As summarized in Table 2, 45 wt% of TOCNF-PEI in alginate hydrogel demonstrated the optimal concentration of TOCNF/PEI to adsorb CR with adsorption capacity for CR (0.95016 mg/g) and removed 95 % of the dye effectively. When concentration of TOCNF/PEI more than 45 wt%, the removal efficiencies did not vary much, indicating that the optimal concentration of TOCNF/PEI to remove CR dye from the test solution is 45 wt%.

Table 2 Adsorption capacity of biocomposite prepared in various concentration of TOCNF-PEI tested for CR.

(TOCNF/PEI) (wt%)	qe (mg/g)	Dye removal (%)
0	0.720	72
5	0.824	82
15	0.836	84
30	0.903	90
45	**0.950**	**95**
60	0.94991	95

The plausible mechanism for the adsorption of CR onto Al/TOCNF-PEI beads was presented in **Figure 4**. As a mentioned before, we utilized these beads as adsorbent for 2 different dyes, CR and MB each representing anionic and cationic dye, respectively. Our adsorbent demonstrated decent adsorption toward Congo red at pH 6. The adsorption capacity improved upon lowering the pH to 3. This observation was not surprising as the nature of our beads were predominantly positive in charge due to the presence of Ca^{2+} cation throughout the beads surface which came from its fabrication process. These Ca^{2+} cations were thought to be responsible for the adsorption process of the adsorbent through an electrostatic attraction with the negatively charged sulfonate moiety of the Congo Red. Moreover, lowering the pH of the system resulted in the protonation of nitrogen of the PEI backbones to form ammonium functionality. The presence of ammonium moiety further increased the electrostatic attraction towards the Congo Red. Hence, the adsorption capacity of the adsorbent was better in lower pH for this dye. On the other hand, adsorption of the beads towards cationic dye Methylene Blue was negligible due to charge incompatibility between the adsorbent and the dye. Both the adsorbent and the Methylene Blue were positively charged. As a consequence, no attraction phenomena occurred.

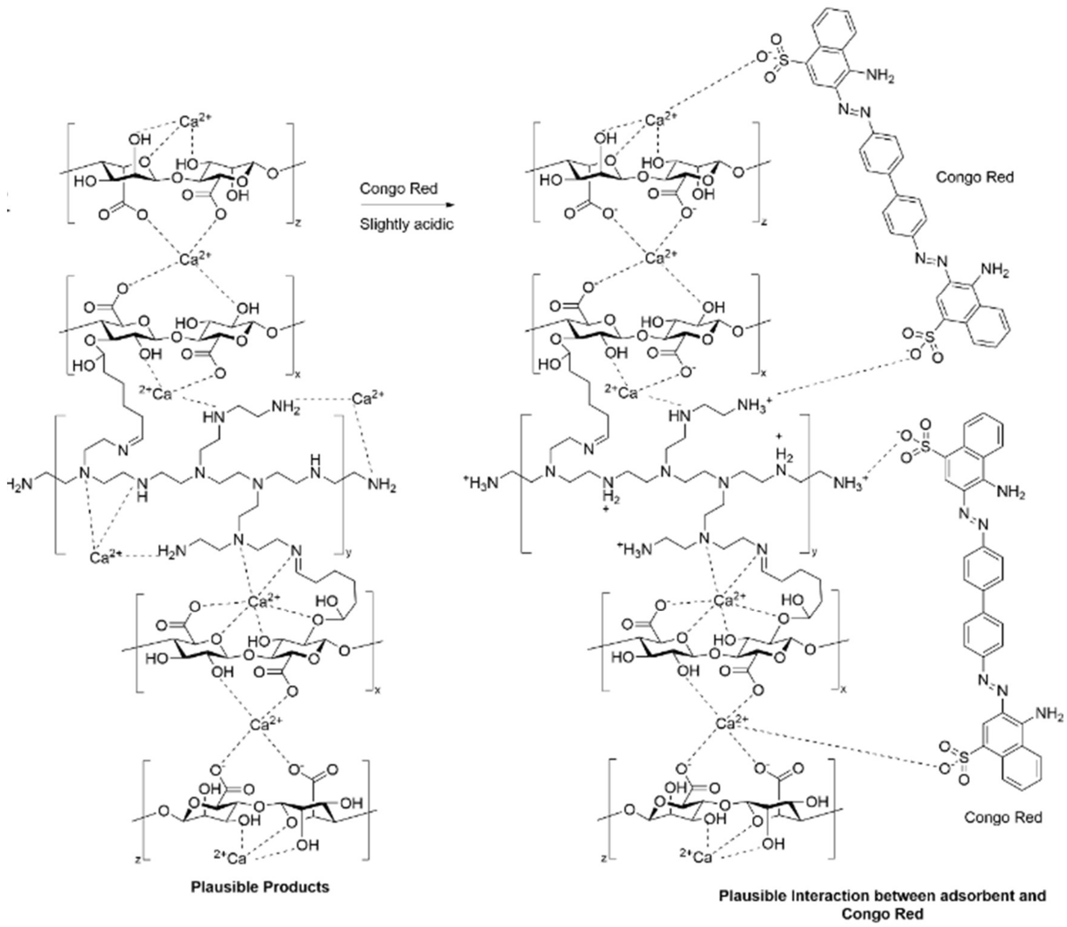

Figure 4 Plausible adsorption mechanism of CR onto beads biocomposite.

Morphology of biocomposite beads

The SEM images of the hydrogel biocomposite before and after the adsorption of Congo Red are shown in **Figures 5(a)** - **5(c)**. It was observed that the adsorption process resulted in substantial alterations to the surface texture of the biocomposite. The dried surface of alginate hydrogel beads exhibited a smooth and nonporous structure (**Figure 5(a)**), which was contrasted with the rough and granular surface of Al/TOCNF-PEI hydrogel beads (**Figure 5(b)**). The surface of dried Al/TOCNF-PEI hydrogel beads exhibited a smooth with wrinkled morphology. However, it was clear from the SEM micrographs that TOCNF/PEI was efficiently dispersed in the hydrogel network, no agglomeration was observed. This may be due to the presence of ammonium groups in TOCNF/PEI, which facilitates a better interaction between TOCNF/PEI and alginate. After the dye was absorbed, a thick coating of dye was seen covering the pores. As a result, the surface of the hydrogel beads displayed a granulated structure (**Figure 5(c)**). This observation indicated that the pores were now filled with dye, which was in good accordance with the findings reported in the literature for similar works [27,29].

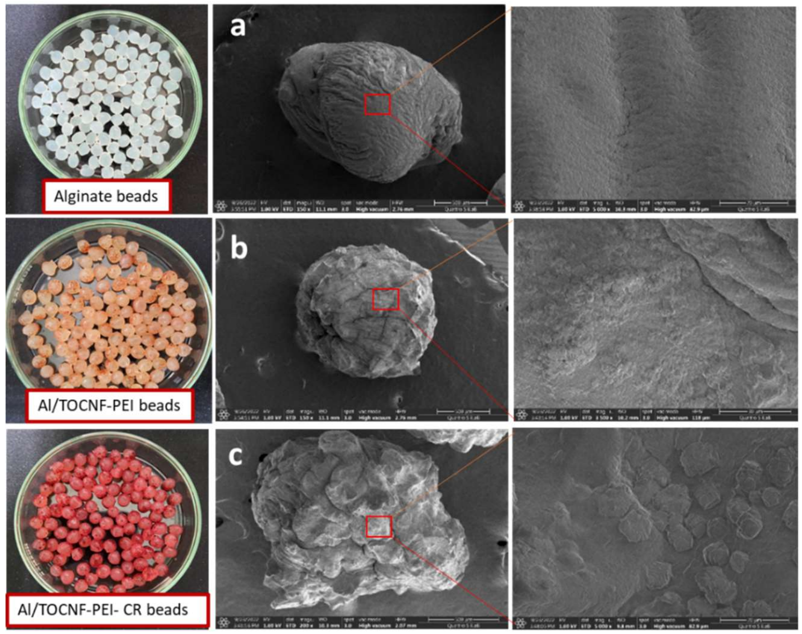

Figure 5 SEM micrograph of a. Alginate beads; b. Al-TOCNF-PEI beads, and c. Al/TOCNF/PEI-CR beads.

Adsorption test

Effect of initial concentration and contact time

Figure 6(a) shows the effect of contact time and initial dye concentration on the adsorption capacity (qt). At the low initial concentration of dye, all the dye ions can interact with the active site of the adsorbent. This means that a high percentage of the dye is removed. In contrast, at high starting dye concentrations, the adsorbent becomes rapidly saturated, resulting in a decrease in the removal. At the beginning of the adsorption process, the adsorption capacity of Al/TOCN-PEI for CR dye increased rapidly with increasing adsorption time. On the surface of the adsorbent material, there are usually a large number of available adsorption sites. When the adsorption process starts, dye molecules from the solution quickly start to swiftly bind to these available sites. This causes a rapid rise in the adsorption capacity during this initial phase. However, as more dye molecules occupy these sites throughout the process of adsorption, the number of available adsorption sites on the adsorbent surface start to decrease. As a result, the adsorption rate decreases, and the adsorption capacity begins to level off. After 60 min of operation, the equilibrium of the adsorption process had almost been attained. Above this time interval, no significant improvement of the rate of dye adsorption was observed due to the saturation of most active sites of the adsorbent [28,30].

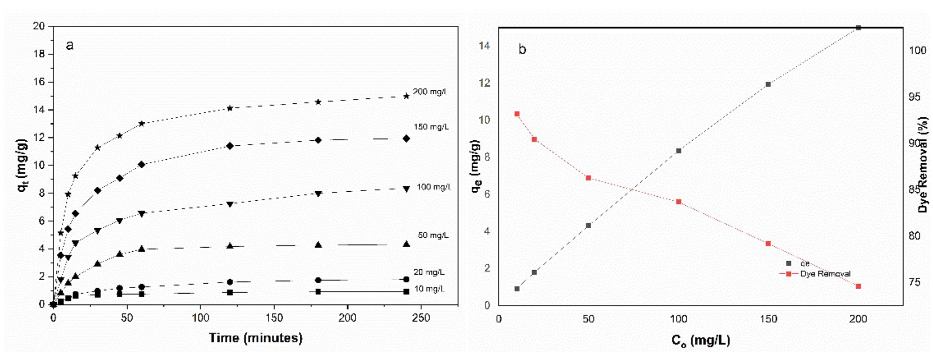

Figure 6 (a) Effect of contact time and initial dye concentration on the adsorption capacity (qt), (b) Effect of initial dye concentration on the adsorption capacity and percentage of dye removal of adsorbents. measured at 10 g/L of adsorbent dosage, RT, and pH 6.

Figure 6(b) depicts the influence of starting dye concentration on the adsorption capacity and dye removal of the adsorbents. The initial concentration of the dye was set between 10 and 200 mg/L. As shown in **Figure 5(a)**, the initial dye concentration altered the adsorbents' capacity and their removal rate. Increase in the initial dye concentration improved the adsorption capacity but decreased the removal rate value. The adsorption procedure performed with an initial dye concentration of 10 mg/L and an adsorbent dose of 10 g/L at room temperature and pH 6 yielded an adsorption capacity of 0.931 mg/g and a removal percentage of 93.17 %. Under the same conditions, increasing the initial dye concentration to 200 mg/L raised the adsorbent capacity to 14.98 mg/g. However, the removal percentage fell to 74.63 %. In the adsorption process, the relationship between adsorption capacity and removal rate with increasing initial dye concentration is influenced by various factors. In this research, at very high initial dye concentrations, the adsorption sites on the adsorbent surface can become saturated. This means that all available sites are occupied, and further increases in dye concentration might not significantly increase the adsorption capacity. However, the removal rate might still decrease due to mass transfer limitations.

Effect of adsorbent dosage

Adsorbent dose is another important factor in the adsorption test that determines the adsorption capacity of an adsorbent. This parameter was used to estimate the suitable amount of adsorbent per unit of treated solution [34]. **Figure 7(a)** showed that as adsorbent dosage increased the uptake of CR dye in solution also increased. The removal percentage of Al/TOCNF-PEI beads towards CR increased from 56.33 to 96.35 % when the adsorbent dosage was increased from 5 to 15 g/L. Likewise, the adsorption capacity increased from 5.633 to 9.630 mg/g. The adsorbent dosage is closely related with the availability of active sites and affects the interaction with the dye. Higher adsorbent dosage makes more active sites that can interact with the dyes and then increase the CR dyes removal. It can be seen at **Figure 7(b)** higher adsorbent dosage resulted in higher adsorption capacity because more adsorbent active sites were available to interact with the dye. A similar tendency was reported by Dinesha *et al.*, where the % of dye removal has increased as the dose has increased [31]

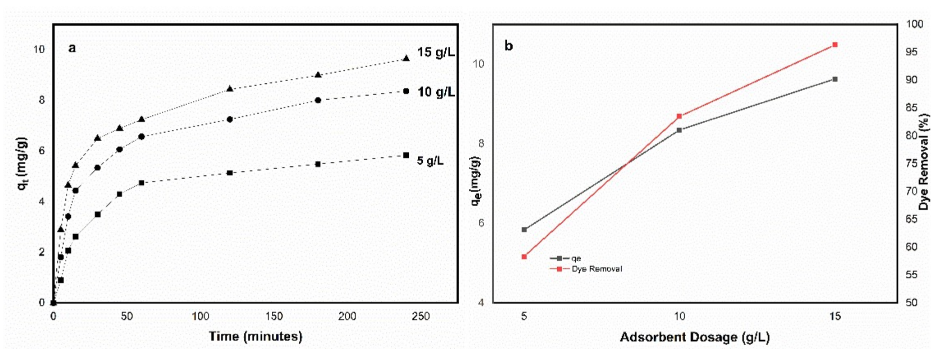

Figure 7 (a) Effect of contact time and adsorbent dosage on the adsorption capacity (qt), (b) Effect of adsorbent dosage on the adsorption capacity and percentage removal of dye. measuring in the initial dye concentration of 100 mg/L, RT, and pH 6.

Effect of pH

The effect of pH on the adsorption capacity and dye removal of CR by the prepared Al/TOCN-PEI hydrogel beads was studied in pH 3, 6, and 9 using 10 g/L of adsorbent in 100 mg/L of CR solution at RT. The results showed that pH had a significant impact on both properties. **Figure 8(a)** showed that a rise in the pH also decreased the adsorption rate. Reduction of the pH of solution caused protonation of amine group in the PEI backbones generating positively charged ammonium functionality, which made interaction with the negatively charged of sulfonate moiety of the CR dye more favorable. As detailed can be seen in in the plausible adsorption mechanism of Al/TOCNF-PEI towards CR (**Figure 3**). At pH 9, the hydroxyl (OH-) ions in the solution competed with the CR anions to bind to the active sites of the adsorbent, resulting in a quicker saturation of the adsorbent and reduction in adsorption capacity and percentage of dye removal. This result in line with study conducted by Khaoula *et al.*, 2019 which use pine park as adsorbent for Congo red and the result shows that the adsorption anionic dyes, such as Congo red, increases as the pH decreases. [4] Furthermore, as demonstrated in **Figure 8(b)**, the CR adsorption on Al/TOCN-PEI hydrogel beads were most effective at pH 3. The amount of CR removed from the solution fell from 95 to 29 % when the pH improved from 3 to 9, followed by decreasing in the adsorption capacity from 9.437 to 2.890 mg/g.

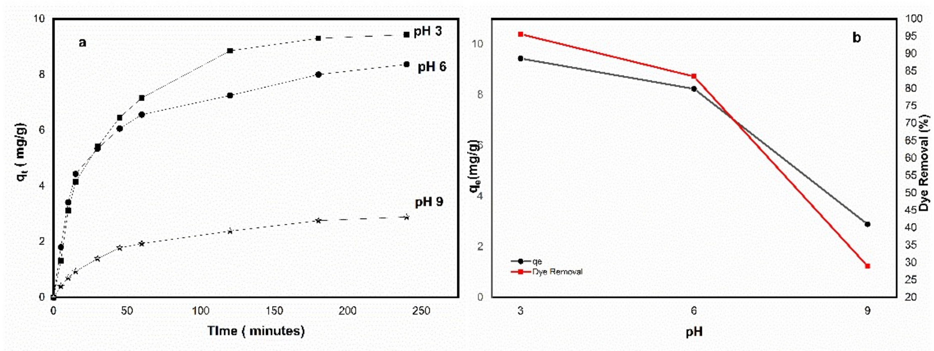

Figure 8 (a) Effect of contact time and pH on the adsorption capacity (qt), (b) Effect of pH on the adsorption capacity and removal percentage of dye, measured in the initial dye concentration of 100 mg/L, the adsorbent dosage of 10 g/L, and at RT.

Adsorption isotherm

Adsorption isotherms were used to investigate the relationship between the amount of CR dye adsorbed onto Al/TOCN-PEI hydrogel beads and the concentration of CR dye in the aqueous phase at the equilibrium state. This parameter was evaluated to determine whether there was a linear relationship between the 2 variables. The results of the Langmuir and Freundlich isotherm analyses, which were performed on the experimental adsorption data for CR dyes, are depicted in **Figure 9**.

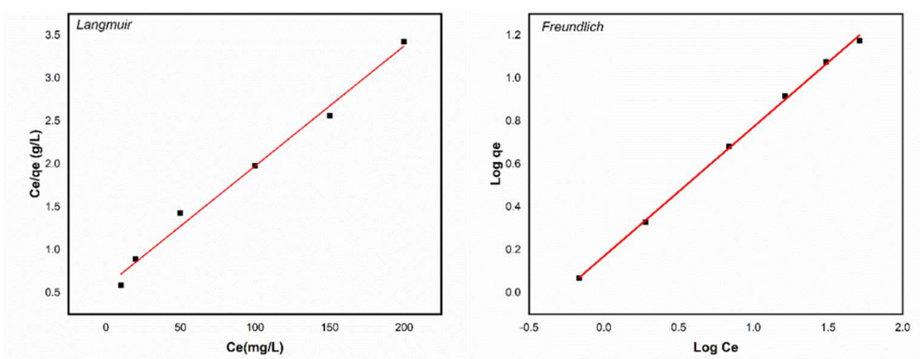

Figure 9 The isotherm model of CR adsorption at various temperatures (a) Langmuir model, (b) Freundlich model, measured in the initial dye concentration (Co) of 100 mg/L, adsorbent dosage of 10 g/L, pH 6, and at RT.

The Langmuir adsorption isotherm model relies on the homogenous surface created by identical active sites and the monolayer adsorption of adsorbate onto the adsorbent surface. In the meanwhile, the Freundlich isotherm model, which is based on multilayer adsorption on a heterogeneous surface, is also employed. The Langmuir model is presented in Eq. (4).

$$qe = \frac{qmaxKCe}{1+KCe} \tag{4}$$

where qe (mg/g) is the amount of adsorbed dye per unit mass of adsorbent, Ce (mg/L) is an unadsorbed dye concentration in solution at equilibrium. q_{max}(mg/g) is the maximum amount of the adsorbed dye per unit mass of adsorbent to form a complete monolayer on the surface bound at high Ce (mg/g). K(L/mg) is a constant related to binding sites affinity. The linear model for Langmuir equation is presented in Eq. (5).

$$\frac{Ce}{qe} = \frac{1}{q_{max}} x\, K + \frac{Ce}{q_{max}} \tag{5}$$

Non-linear and linear mathematical models of Freundlich adsorption isotherms are formulated according to Eqs. (6) - (7).

$$qe = K_F \, Ce^{1/n} \tag{6}$$

$$\log qe = \log K_F + \frac{1}{n}\log Ce \tag{7}$$

where, qe is the maximum quantity of dye absorbed per mass of adsorbent in equilibrium (mg/g), Ce is the equilibrium concentration of dye in solution (mg/L), and K_F is the Freundlich constant, and n is a heterogeneity factor. The K_F value is associated with the relative adsorption capacity of the adsorbent (mg/g). The K_F and n value are determined from the intercept and slope of the linier plot log qe versus log Ce (**Figure 9(b)**).

Table 3 The model parameters of Langmuir and Freundlich isotherms at initial dye concentration (Co) of 100 mg/L, adsorbent dosage of 10 g/L, RT, and pH 6.0.

Langmuir	
q_{max} (mg/g)	71.42857
K_L	0.02436
R^2	0.97744
Freundlich	
K_F	1.4774
n	0.60262
R^2	0.99879

Table 3 provides a concise summary of the model parameters together with the linear correlation coefficient (R^2). The correlation coefficient data showed that the Freundlich isotherm provided a better fit for the experimental data than the Langmuir model did. Based on the result on this research, multiple layers of adsorbate molecules can be adsorbed onto the surface of Al/TOCNF-PEI45 beads. Assumes heterogeneity in the adsorption sites and energy distribution. However, in Langmuir isotherm, the adsorption process assumes as a monolayer adsorption, meaning only one layer of adsorbate molecules can attach to the adsorbent surface.

Adsorption kinetic

Studies of adsorption kinetics help us to understand the adsorption rate as well as the mechanism controlling the process. The pseudo-first order and the pseudo-second-order kinetics models were used to assess the experimental data so that the adsorption kinetics of CR dyes on Al-TOCN/PEI hydrogel beads could be clarified. **Figure 10** displays the fitting of linear forms for the pseudo-first-order kinetic model and the pseudo-second-order kinetic model. Comparing the adsorption capacity and R^2 values of both models, it was evident that the pseudo-first-order kinetic model was not well suitable for simulating the CR dye adsorption onto the produced adsorbent. Moreover, the pseudo-second-order kinetic model gave $R^2 > 0.99$ offering stronger correlation of the experimental data to this model.

The pseudo second-order kinetic model is often more suitable for chemisorption processes or adsorption mechanisms in which electrons are shared or exchanged between the adsorbate and adsorbent. Assuming that the rate of adsorption is directly proportional to the square of the distinction between the equilibrium adsorption and the adsorption at time implies that the rate of adsorption becomes more significant as approaches. On the other hand, for the pseudo first-order, the adsorption rate would decrease as the adsorption process approaches equilibrium. The pseudo first-order kinetic model is well-suited to describe adsorption processes that involve physical adsorption or where the rate-limiting step is surface diffusion.

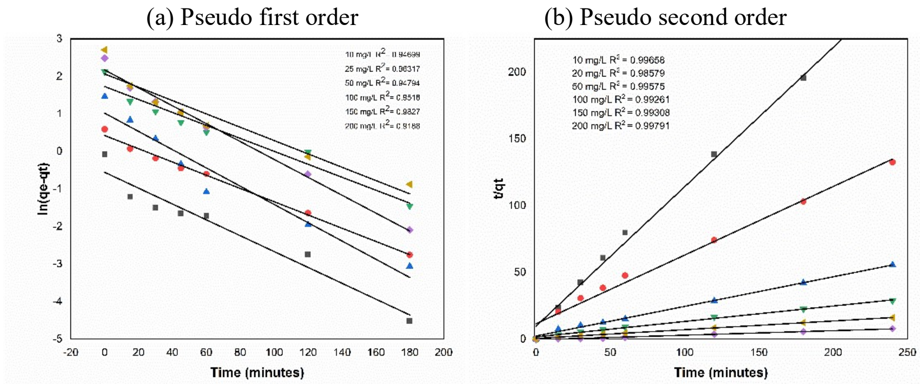

Figure 10 Plots of adsorption kinetics (a) pseudo-first-order model, (b) pseudo-second-order model at different CR concentrations, measured at adsorbent dosage of 10 g/L, pH 6.0, and RT.

Future prospect of Al/TOCNF-PEI hydrogel beads as adsorbent

The Al/TOCNF-PEI hydrogel beads have great potential as an eco-friendly adsorbent for CR removal. This adsorbent also can also be used to adsorb other toxic dyes with anionic charge properties based on electrostatic interactions. The Hydrogel beads could be further investigated for advanced water treatment applications, such as the removal of contaminants including pharmaceuticals, personal care products, and microplastics. Moreover, Hydrogel beads' selectivity and adsorption capability for specific pollutants could be improved through research. Furthermore, the adsorbent could be tailored for efficient and selective removal of heavy metals from wastewater. Future research might involve developing hybrid adsorbents by incorporating other materials to enhance metal adsorption and investigating the regeneration potential for metal recovery. Hydrogel beads could be used for in-situ environmental remediation, such as groundwater or soil treatment to remove pollutants or contaminants. Optimizing the physical and chemical features of the beads for successful pollution removal and long-term stability could be the subject of future research.

In terms of large production of the adsorbent, there are potential challenges in scaling up the production of the materials for large scale dyes removal applications. While biocomposite beads provide sustainable and eco-friendly solutions for dye removal, the transition from laboratory-scale to industrial-scale production involves many considerations and potential obstacles. Such as variability in raw materials can lead to inconsistencies in bead properties, affecting their adsorption capacity and performance. In addition, we also need to ensure the compatibility and stability of the materials over large volumes, which is difficult because leading to changes in bead properties and performance and then achieving consistent bead size, shape, and distribution becomes more complex as the production volume increases.

Conclusions

We have successfully fabricated an eco-friendly adsorbent for the removal of hazardous dye from aqueous medium. Testing the adsorbent for 2 types of dyes; anionic dyes of Congo red and cationic dye of Methylene blue showed that the Alginate/TOCNF-PEI45 biocomposite bead could act as an adsorbent for the CR dye and does not work with cationic dyes. The initial dye concentration, contact time, adsorbent dose, and pH solution had effects on the adsorption capacity and removal percentage of biocomposite beads. The highest CR adsorption capacity was attained under circumstances of lower initial dye concentration, greater adsorbent dose, and lower pH. In the meanwhile, high removal percentage was achieved at low starting dye concentration and pH, and high adsorbent dose. The longer the contact duration, the greater the adsorption capacity and elimination percentage. The adsorption mechanism of our adsorbent agreed with the Freundlich isotherm model, following the pseudo-second-order adsorption kinetic model.

Acknowledgements

The authors acknowledge for *Rumah Program Material Maju* 2022 from Research Organization of Nanomaterial and Advanced Material-BRIN and the facilities, scientific, and technical support form Advanced Characterization Laboratories Cibinong - Integrated Laboratory of Bioproduct, National Research and Innovation Agency, Indonesia, through E- Layanan Sains, Badan Riset dan Inovasi Nasional (BRIN), Indonesia.

References

[1] R Mia, M Selim, AM Shamim, M Chowdhury, S Sultana, M Armin, M Hossain, R Akter, S Dey and H Naznin. Review on various types of pollution problem in textile dyeing & printing industries of Bangladesh and recommandation for mitigation. *J. Textil. Eng. Fashion Tech.* 2019; **5**, 220-6.

[2] M Berradi, R Hsissou, M Khudhair, M Assouag, O Cherkaoui, A El Bachiri and A El Harfi. Textile finishing dyes and their impact on aquatic environs. *Heliyon* 2019; **5**, e02711.

[3] PM Dellamatrice, ME Silva-Stenico, LABD Moraes, MF Fiore and RTR Monteiro. Degradation of textile dyes by cyanobacteria. *Braz. J. Microbiol.* 2017; **48**, 25-31.

[4] K Litefti, MS Freire, M Stitou and J González-Álvarez. Adsorption of an anionic dye (Congo red) from aqueous solutions by pine bark. *Sci. Rep.* 2019; **9**, 16530.

[5] S Radoor, J Karayil, J Parameswaranpillai and S Siengchin. Removal of anionic dye Congo red from aqueous environment using polyvinyl alcohol/sodium alginate/ZSM-5 zeolite membrane. *Sci. Rep.* 2020; **10**, 15452.

[6] CQ Ruan, M Strømme and J Lindh. Preparation of porous 2,3-dialdehyde cellulose beads crosslinked with chitosan and their application in adsorption of congo red dye. *Carbohydr. Polymer.* 2018; **181**, 200-7.

[7] H Anwer, A Mahmood, J Lee, KH Kim, JW Park and ACK Yip. Photocatalysts for degradation of dyes in industrial effluents: Opportunities and challenges. *Nano Res.* 2019; **12**, 955-72.

[8] L Urbina, O Guaresti, J Requies, N Gabilondo, A Eceiza, MA Corcuera and A Retegi. Design of reusable novel membranes based on bacterial cellulose and chitosan for the filtration of copper in wastewaters. *Carbohydr. Polymer.* 2018; **193**, 362-72.

[9] S Khamparia and DK Jaspal. Adsorption in combination with ozonation for the treatment of textile wastewater: A critical review. *Front. Environ. Sci. Eng.* 2017; **11**, 8.

[10] JA González, ME Villanueva, LL Piehl and GJ Copello. Development of a chitin/graphene oxide hybrid composite for the removal of pollutant dyes: Adsorption and desorption study. *Chem. Eng. J.* 2015; **280**, 41-8.

[11] Z Yu, C Hu, AB Dichiara, W Jiang and J Gu. Cellulose nanofibril/carbon nanomaterial hybrid aerogels for adsorption removal of cationic and anionic organic dyes. *Nanomaterials* 2020; **10**, 169.

[12] C Phaenark, T Jantrasakul, P Paejaroen, S Chunchob and W Sawangproh. Sugarcane bagasse and corn stalk biomass as a potential sorbent for the removal of Pb (II) and Cd (II) from aqueous solutions. *Trends Sci.* 2023; **20**, 6221.

[13] X Wei, T Huang, J Nie, JH Yang, XD Qi, ZW Zhou and Y Wang. Bio-inspired functionalization of microcrystalline cellulose aerogel with high adsorption performance toward dyes. *Carbohydr. Polymer.* 2018; **198**, 546-55.

[14] A Pei, N Butchosa, LA Berglund and Q Zhou. Surface quaternized cellulose nanofibrils with high water absorbency and adsorption capacity for anionic dyes. *Soft Matter* 2013; **9**, 2047-55.

[15] MTMH Hamad and MSS Saied. Kinetic studies of congo red dye adsorption by immobilized aspergillus niger on alginate. *Appl. Water Sci.* 2021; **11**, 35.

[16] N Ayawei, SS Angaye, D Wankasi and ED Dikio. Synthesis, characterization and application of Mg/Al layered double hydroxide for the degradation of congo red in aqueous solution. *Open J. Phys. Chem.* 2015; **5**, 56-70.

[17] S Asadi, S Eris and S Azizian. Alginate-based hydrogel beads as a biocompatible and efficient adsorbent for dye removal from aqueous solutions. *ACS Omega* 2018; **3**, 15140-8.

[18] N Lin, C Bruzzese and A Dufresne. TEMPO-oxidized nanocellulose participating as crosslinking aid for alginate-based sponges. *ACS Appl. Mater. Interfac.* 2012; **4**, 4948-59.

[19] RE Abou-Zeid, KA Ali, RMA Gawad, KH Kamal, S Kamel and R Khiari. Removal of cu (Ii), pb(ii), mg(ii), and fe(ii) by adsorption onto alginate/nanocellulose beads as bio-sorbent. *J. Renew. Mater.* 2021; **9**, 601-13.

[20] E Syafri, Jamaluddin, NH Sari, M Mahardika, P Amanda and RA Ilyas. Isolation and characterization of cellulose nanofibers from Agave gigantea by chemical-mechanical treatment. *Int. J. Biol. Macromol.* 2022; **200**, 25-33.

[21] P Amanda, S Nabila, N Qonita, RS Ningrum, Ismadi and N Masruchin. The properties of OPEFB cellulose nanofibrils produced by a different mode of ultrafine grinding. *IOP Conf. Ser. Earth Environ. Sci.* 2021; **891**, 012016.

[22] B Yuan, L Li, V Murugadoss, S Vupputuri, J Wang, N Alikhani and Z Guo. Nanocellulose-based composite materials for wastewater treatment and waste-oil remediation. *ES Food Agroforestry* 2020; **1**, 41-52.

[23] JN Putro, A Kurniawan, S Ismadji and YH Ju. Nanocellulose based biosorbents for wastewater treatment: Study of isotherm, kinetic, thermodynamic and reusability. *Environ. Nanotechnology Monit. Manag.* 2017; **8**, 134-49.
[24] DA Gopakumar, V Arumughan, D Pasquini, SY Leu, HPSA Khalil and S Thomas. Chapter 3 - nanocellulose-based membranes for water purification. *Nanoscale Mater. Water Purif.* 2019; **2019**, 59-85.
[25] Z Karim, S Claudpierre, M Grahn, K Oksman and AP Mathew. Nanocellulose based functional membranes for water cleaning: Tailoring of mechanical properties, porosity and metal ion capture. *J. Membr. Sci.* 2016; **514**, 418-28.
[26] N Zhang, GL Zang, C Shi, HQ Yu and GP Sheng. A novel adsorbent TEMPO-mediated oxidized cellulose nanofibrils modified with PEI: Preparation, characterization, and application for Cu (II) removal. *J. Hazard. Mater.* 2016; **316**, 11-8.
[27] DM Guo, QD An, ZY Xiao, SR Zhai and Z Shi. Polyethylenimine-functionalized cellulose aerogel beads for efficient dynamic removal of chromium (VI) from aqueous solution. *RSC Adv.* 2017; **7**, 54039-52.
[28] N Masruchin, P Amanda, WB Kusumaningrum, L Suryanegara and A Nuryawan. Particle size distribution and yield analysis of different charged cellulose nanofibrils obtained by TEMPO-mediated oxidation. *IOP Conf. Ser. Earth Environ. Sci.* 2020; **572**, 012045.
[29] N Masruchin, YD Kurniawan, SS Kusumah, P Amanda, L Suryanegara and A Nuryawan. TEMPO-mediated oxidation cellulose pulp modified with Monosodium Glutamate (MSG). *IOP Conf. Ser. Earth Environ. Sci.* 2019; **374**, 012010.
[30] D Sartika, K Syamsu, E Warsiki, F Fahma and IW Arnata. Nanocrystalline cellulose from kapok fiber (Ceiba pentandra) and its reinforcement effect on alginate hydrogel bead. *Starch* 2021; **73**, 2100033.
[31] R Si, C Wu, D Yu, Q Ding and R Li. Novel TEMPO-oxidized cellulose nanofiber/polyvinyl alcohol/polyethyleneimine nanoparticles for Cu2+ removal in water. *Cellulose* 2021; **28**, 10999-1011.
[32] J Supramaniam, R Adnan, NHM Kaus and R Bushra. Magnetic nanocellulose alginate hydrogel beads as potential drug delivery system. *Int. J. Biol. Macromol.* 2017; **118**, 640-8.
[33] IW Arnata, Suprihatin, F Fahma, N Richana and TC Sunarti. Adsorption of anionic congo red dye by using cellulose from sago frond. *Pollut. Res.* 2019; **38**, 557-67.
[34] KS Padmavathy, G Madhu and PV Haseena. A study on effects of pH, adsorbent dosage, time, initial concentration and adsorption isotherm study for the removal of hexavalent chromium (Cr (VI)) from wastewater by magnetite nanoparticles. *Proc. Tech.* 2016; **24**, 585-94.
[35] BL Dinesha, S Hiregoudar, U Nidoni, KT Ramappa, AT Dandekar and SV Ganachari. Adsorption modelling and fixed-bed column study on milk processing industry wastewater treatment using chitosan zinc-oxide nano-adsorbent–coated sand filter bed. *Environ. Sci. Pollut. Res.* 2023; **30**, 37547-69.